Neutrosophic Birnbaum-Saunders distribution with applications

Mansooreh Razmkhah[a,*], Mohammad Arashi[a,b], Andriette Bekker[b], Filipe J. Marques[c]

[a]*Department of Statistics, Faculty of Mathematical Sciences, Ferdowsi University of Mashhad, Manshhad, Iran*
[b]*Department of Statistics, Uinversity of Pretoria, Pretoria, South Africa*
[c]*Department of Mathematics and Center for Mathematics and Applications (NOVA Math), NOVA School of Science and Technology, Portugal*

Abstract

This paper presents an extension of the Birnbaum-Saunders distribution through the incorporation of neutrosophic concepts, aimed at effectively addressing data that is characterized by imprecision, uncertainty, and incompleteness. Our model delivers maximum likelihood parameter estimates, effectively capturing the complete spectrum of interval-based values without compromise. We showcase its benefits in industrial and environmental applications, emphasizing its effectiveness in analyzing uncertain data within real-world scenarios, surpassing traditional statistical methods.

Keywords:
Air pollution data, Birnbaum-Saunders distribution, environmental data analysis, fatigue life data, industrial data modelling, indeterminacy, maximum likelihood estimation, neutrosophic random variables, nitrogen oxides emissions.

1. Introduction

A key benefit of neutrosophic statistics is its flexibility - it extends classical methods while remaining compatible with precise data. In uncertain scenarios, it considers both variability and indeterminacy, offering deeper insights than traditional models. When applied to precise datasets, neutrosophic models revert to classical forms, ensuring a seamless transition between certainty and uncertainty. This versatility makes neutrosophic models particularly valuable in modern data analysis. For a comprehensive introduction to neutrosophic statistics, readers may refer to [1].

*Corresponding author:
Email address: ma.razmkhah@alumni.um.ac.ir (Mansooreh Razmkhah)

Recent years have seen the development of neutrosophic versions of several classical distributions. Alhabib et al. [2] studied the neutrosophic Poisson, exponential, and uniform distributions, while Alhasan and Smarandache [3] developed the neutrosophic Weibull distribution. Alduais and Khan [4] investigated the neutrosophic gamma distribution and its applications. Norouzirad et al. [5] introduced the neutrosophic generalized Rayleigh distribution. Other contributions include the neutrosophic extension of the Maxwell model [6], the Kumaraswamy distribution [7], the log-normal distribution [8], the generalized exponential distribution [9], the Beta distribution [10], the generalized Pareto distribution [11], and the Burr-III distribution [12]. The models illustrate the effectiveness of neutrosophic frameworks in addressing uncertainty across diverse fields, such as engineering and environmental science.

Building on these advancements, this paper proposes the Neutrosophic Birnbaum-Saunders Distribution (NBSD), an extension of the classical Birnbaum-Saunders Distribution (BSD) tailored for imprecise and indeterminate datasets. Given the BSD's well-established role in modelling fatigue life data, it serves as a natural foundation for advancing neutrosophic statistics, offering a more robust framework for applications in reliability engineering and environmental monitoring.

Although some studies acknowledge data imprecision and propose models based on intervals, their practical computations often deviate from the stated theoretical framework. Typically, they apply classical statistical methods separately to the lower and upper bounds of the intervals and then combine the results into a final interval. This approach overlooks the internal structure of interval data and may lead to the loss of some information. In contrast, our method performs modeling and computations directly on the entire data interval, preserving the richness of the information and yielding more representative and accurate results under uncertainty. On the other hand, [13] introduced a different model for evaluating imprecise data, in which an uncertainty index is added to the probability density function. This differs from our approach, where the neutrosophic density is directly computed across the entire interval of imprecise data. Our method leads to a more comprehensive representation of uncertainty and preserves a fuller statistical interpretation of the data. In addition, it constructs a density interval that retains its statistical meaning, providing a precise and information-preserving representation of uncertainty. Unlike traditional methods that simplify intervals, the proposed method computes statistical measures directly over the entire interval. This preserves the richness of the original data and delivers more accurate interval-based estimates. Moreover, since it involves minimal modifications to the original density function, the approach is particularly effective in modelling complex data and capturing subtle statistical features with greater accuracy.

The main novel contributions and areas of application of this paper are as follows:

- A new statistical model is introduced: the neutrosophic Birnbaum-Saunders distribution, specifically designed for analyzing imprecise data presented in the form of intervals.
- A parameter estimation procedure is developed that directly operates on the full interval data, without reducing them to point estimates, thereby maintaining the integrity of the uncertainty in the data.
- It is shown that preserving the full interval information leads to more reliable and interpretable statistical inference.
- The methodology is applied to a real-world environmental dataset with imprecise values, confirming its practicality and effectiveness in handling real data with interval uncertainty.
- The proposed framework differs fundamentally from many existing approaches, which either simplify interval data or treat the bounds independently. In contrast, the entire interval is modeled as a whole, capturing its internal structure.
- This work opens up new possibilities for robust statistical modelling in domains where data imprecision is unavoidable, including environmental science, reliability analysis, and engineering systems.
- The relevant R codes used for the estimation procedures, simulation studies, and data analysis are fully provided in a public GitHub repository., facilitating reproducibility and practical application of the proposed methods.

The paper is organized as follows: Section 2 presents a description of the BSD, followed by the introduction of the NBSD in Section 3. Section 4 provides an overview of the statistical characteristics of the NBSD. Section 5 explains the estimation procedure for neutrosophic parameters. A simulation study is conducted in Section 6. Section 7 includes a comparative evaluation based on simulated data. Section 8 showcases practical applications of the NBSD with real-world datasets, followed by a comparative analysis with two other candidate models. Section 9 presents a direct comparison of the proposed method with an alternative model using a real dataset. Finally, Section 10 summarizes the key findings, implications, and practical applications, highlighting the extension of the BSD for data analysis under varying levels of indeterminacy.

2. Birnbaum-Saunders distribution

Out of all statistical distributions, the normal distribution stands out as the most commonly utilized in practical applications. Various new distributions have emerged

by modifying the normal distribution through transformations, mainly because of its mathematical tractability, well-known properties, and its natural appearance in many real-world phenomena due to the Central Limit Theorem. The two-parameter BSD is an example, created by applying a monotone transformation to the standard normal random variable. This distribution is specifically designed to model the fatigue life of metals subjected to cyclic stress, often referred to as the fatigue-life distribution.

A random variable T follows the BSD if it can be expressed as

$$T = \beta\left(\frac{\alpha}{2}Z + \sqrt{\left(\frac{\alpha}{2}Z\right)^2 + 1}\right)^2; \quad Z = \frac{1}{\alpha}\left[\sqrt{\frac{T}{\beta}} - \sqrt{\frac{\beta}{T}}\right] \sim \mathcal{N}(0,1), \tag{1}$$

where $\alpha > 0$, and $\beta > 0$ are shape and scale parameters, respectively. The cumulative distribution function (CDF) is defined as

$$F(t;\alpha,\beta) = \Phi\left(\frac{1}{\alpha}\left(\sqrt{\frac{t}{\beta}} - \sqrt{\frac{\beta}{t}}\right)\right), \quad t > 0, \quad \alpha,\beta > 0 \tag{2}$$

where $\Phi(\cdot)$ denotes the standard normal CDF. The associated probability density function (PDF) is given by

$$f(t;\alpha,\beta) = \frac{1}{\sqrt{2\pi}}\exp\left\{-\frac{1}{2\alpha^2}\left(\frac{t}{\beta} + \frac{\beta}{t} - 2\right)\right\}\frac{t^{\frac{-3}{2}}(t+\beta)}{2\alpha\sqrt{\beta}}, \quad 0 < t < \infty, \quad \alpha,\beta > 0. \tag{3}$$

Balakrishnan and Kundu [14] provided a detailed review of the progress of all Birnbaum-Saunders models.

3. Neutrosophic Birnbaum-Saunders distribution

Let $T_N \in [T_L, T_U]$ be a neutrosophic random variable. We assume $T_N \sim NBS(\alpha_N, \beta_N)$ and in general say T_N follows a NBSD with neutrosophic shape parameter $\alpha_N \in [\alpha_L, \alpha_U]$ and neutrosophic scale parameter $\beta_N \in [\beta_L, \beta_U]$. Then, the associated neutrosophic PDF and CDF can be expressed as follows respectively

$$f(t_N;\alpha_N,\beta_N) = \frac{1}{\sqrt{2\pi}}\exp\left(-\frac{1}{2{\alpha_N}^2}\left[\frac{t}{\beta_N} + \frac{\beta_N}{t} - 2\right]\right)\frac{t_N^{\frac{-3}{2}}[t_N+\beta_N]}{2\alpha_N\sqrt{\beta_N}}, \quad 0 < t_N < \infty, \quad \alpha_N,\beta_N > 0 \tag{4}$$

and

$$F(t_N;\alpha_N,\beta_N) = \Phi\left[\frac{1}{\alpha_N}\left\{\left(\frac{t_N}{\beta_N}\right)^{\frac{1}{2}} - \left(\frac{\beta_N}{t_N}\right)^{\frac{1}{2}}\right\}\right], \quad t_N > 0, \quad \alpha_N > 0, \quad \beta_N > 0. \tag{5}$$

Within real-world scenarios, every piece of information possesses the capacity to include a certain level of uncertainty, and the values of parameters may likewise be subject to uncertainty. Obviously, when there is no uncertainty about any of the sample values or parameters, the lower and upper bounds become equal and the model reduces to classical model.

If $T_N \sim \text{NBS}(\alpha_N, \beta_N)$, the survival and hazard functions of the NBSD are respectively given by

$$s(t_N; \alpha_N, \beta_N) = 1 - \Phi\left[\frac{1}{\alpha_N}\left\{\left(\frac{t_N}{\beta_N}\right)^{\frac{1}{2}} - \left(\frac{\beta_N}{t_N}\right)^{\frac{1}{2}}\right\}\right] \tag{6}$$

and

$$h(t_N; \alpha_N, \beta_N) = \frac{f(t_N; \alpha_N, \beta_N)}{1 - F(t_N; \alpha_N, \beta_N)}, \quad t > 0. \tag{7}$$

Evaluating these functions is complex due to the imprecision in either the parameters of the distribution or input data. A common approach in neutrosophic computations is to either apply a linear combination of the lower and upper bounds of the interval, effectively reducing the problem to classical statistics, or to compute statistical measures separately at the lower and upper bounds and report the results as an interval. However, both methods lead to a loss of information, as they do not fully account for the entire range of values within the neutrosophic interval. To ensure accurate and comprehensive results, it is essential to cover the entire neutrosophic interval and compute the probability values across all possible parameter values within the given domain. The most reliable approach for this computation is to determine the minimum and maximum values of the function over the interval, ensuring that no information is lost in the process. This purpose is achieved by using the `optim` function in R with the L-BFGS-B method [15]. The following example further illustrates this process.

The fatigue lifespan in hours of a ball bearing, T_N, follows a NBSD with indeterminate parameters as $T_N \sim NBS([0.08, 0.09], [179.5, 181])$. The probability that the fatigue lifespan is more than 170 hours is calculated from (6)

$$\begin{aligned} s(170; \alpha_N, \beta_N) &= 1 - \Phi\left[\frac{1}{[0.08, 0.09]}\left\{\left(\frac{170}{[179.5, 181]}\right)^{\frac{1}{2}} - \left(\frac{[179.5, 181]}{170}\right)^{\frac{1}{2}}\right\}\right] \\ &= [0.7271649, 0.7834391]. \end{aligned}$$

Then, the probability of the fatigue lifespan exceeding 170 hours is between 72.7% and 78.3%, accounting for the uncertainty in the parameters.

Figure 1 illustrates how PDF values of NBSD change with different neutrosophic scale and/or shape parameters. Figures 2 and 3 display the CDF and hazard functions

of the NBSD, respectively. Black curves in all plots show the function values in lower and upper boundary of neutrosophic parameters, and the coloured areas represent the function values as parameters change through indeterminacy intervals.

4. Properties of the NBSD

This section presents key statistical properties - such as central tendency, variability, and shape - for the NBSD, leveraging interval values in the neutrosophic framework to capture uncertainty. When $T_N \sim NBS(\alpha_N, \beta_N)$, by using the relation in (1), and different moments of the standard normal random variable, the non-central moments of T_N, for integer r, are

$$\mathbb{E}\left(T_N^r\right) = \beta_N^r \sum_{j=0}^{r} \binom{2r}{2j} \sum_{i=0}^{j} \binom{j}{i} \frac{(2r-2j+2i)!}{2^{r-j+i}(r-j+i)!} \left(\frac{\alpha_N}{2}\right)^{2r-2j+2i}. \tag{8}$$

All moments are derived from the central moments in (8). The core statistical properties, as calculated for the NBSD, are summarized in Table 1.

Table 1: Statistical characteristics of the NBSD under the neutrosophic framework.

Mean	$\beta_N \left(1 + \frac{{\alpha_N}^2}{2}\right)$
Variance	$(\alpha_N \beta_N)^2 \left(1 + \frac{5}{4}{\alpha_N}^2\right)$
Coefficient of variation	$\frac{\sqrt{5\alpha_N^4 + 4\alpha_N^2}}{\alpha_N^2 + 2}$
Skewness	$\frac{16{\alpha_N}^2\left(11{\alpha_N}^2+6\right)}{\left(5{\alpha_N}^2+4\right)^3}$
Kurtosis	$3 + \frac{6{\alpha_N}^2\left(93{\alpha_N}^2+40\right)}{\left(5{\alpha_N}^2+4\right)^2}$

The median of the distribution is equal to β_N. As $\alpha_N \to 0$, the coefficient of kurtosis converges to 3, indicating that the behavior of the NBSD approximates that of a neutrosophic normal distribution with mean and variance around β_N and $\beta_N^2\alpha_N^2$, respectively.

Determining statistical characteristics in the neutrosophic framework requires identifying extreme values across the interval-defined parameter space, α_N and β_N. This process accounts for parameter uncertainty and is carried out using the `optim` function in R with the L-BFGS-B method. Table 2 presents the descriptive characteristics for various values of β_N and α_N under the neutrosophic framework. The results show that with a fixed β_N, increasing α_N leads to higher values for mean and variance, reflecting the effect of greater uncertainty. Conversely, with a fixed α_N, higher values

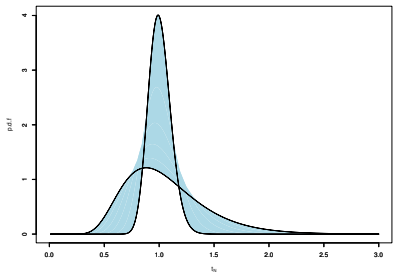

$\beta = 1, \alpha_N \in [0.1, 0.35]$

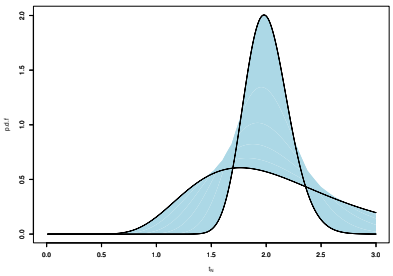

$\beta = 2, \alpha_N \in [0.1, 0.35]$

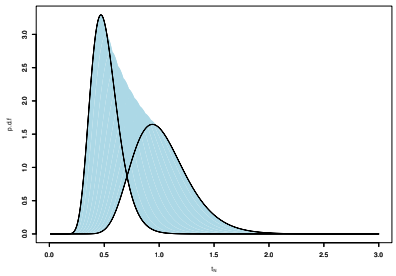

$\alpha = 0.25, \beta_N \in [0.5, 1]$

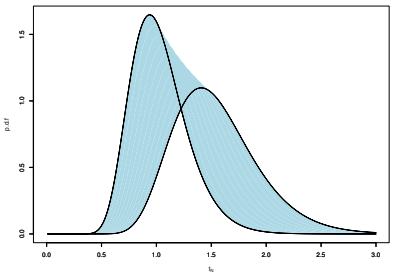

$\alpha = 0.25, \beta_N \in [1, 1.5]$

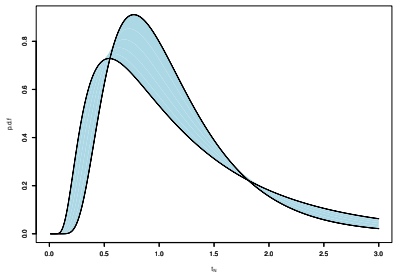

$\beta = 1, \alpha_N \in [0.5, 0.75]$

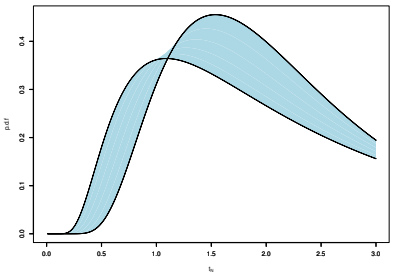

$\beta = 2, \alpha_N \in [0.5, 0.75]$

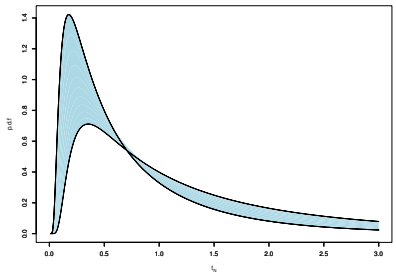

$\alpha = 1, \beta_N \in [0.5, 1]$

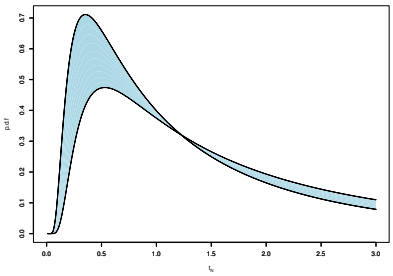

$\alpha = 1, \beta_N \in [1, 1.5]$

Figure 1: The PDF plots of NBSD against different neutrosophic parameters' values.

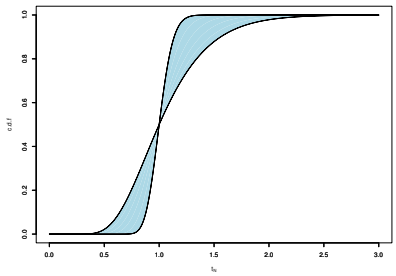

$\beta = 1, \alpha_N \in [0.1, 0.35]$

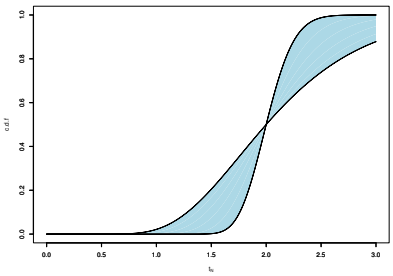

$\beta = 2, \alpha_N \in [0.1, 0.35]$

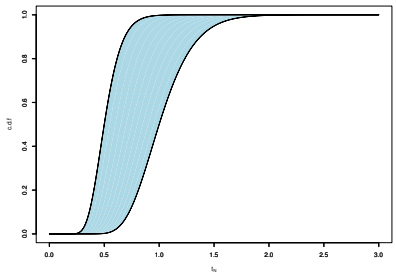

$\alpha = 0.25, \beta_N \in [0.5, 1]$

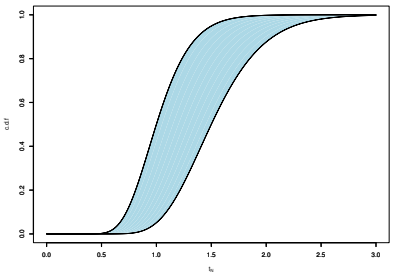

$\alpha = 0.25, \beta_N \in [1, 1.5]$

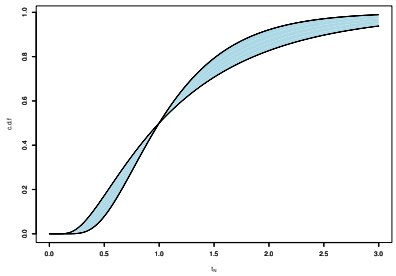

$\beta = 1, \alpha_N \in [0.5, 0.75]$

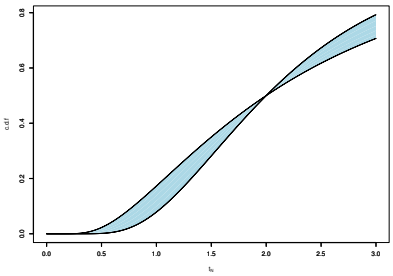

$\beta = 2, \alpha_N \in [0.5, 0.75]$

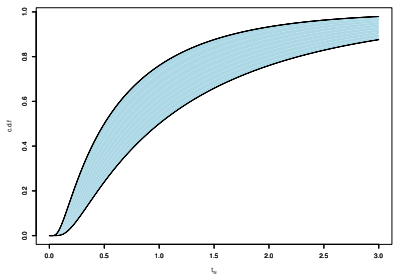

$\alpha = 1, \beta_N \in [0.5, 1]$

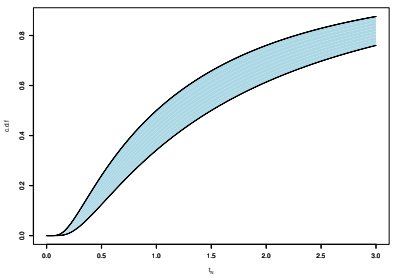

$\alpha = 1, \beta_N \in [1, 1.5]$

Figure 2: The CDF plots of NBSD against different neutrosophic parameters' values.

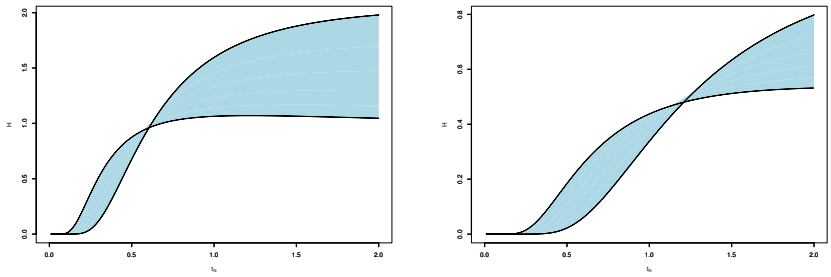

$\beta = 1, \alpha_N \in [0.5, 0.75]$ $\beta = 2, \alpha_N \in [0.5, 0.75]$

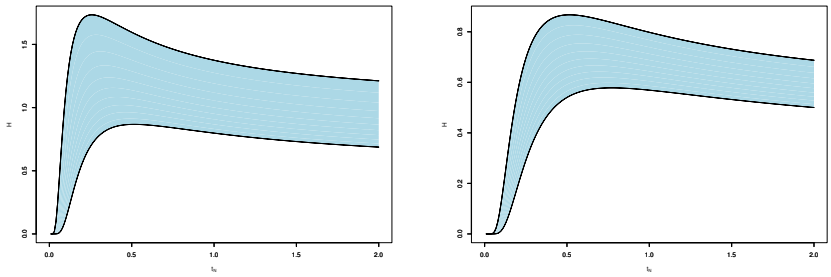

$\alpha = 1, \beta_N \in [0.5, 1]$ $\alpha = 1, \beta_N \in [1, 1.5]$

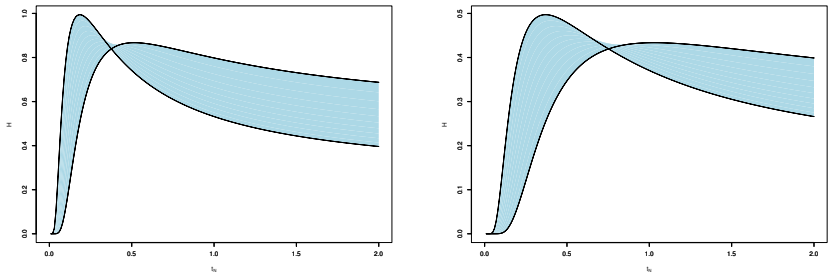

$\beta = 1, \alpha_N \in [1, 1.5]$ $\beta = 2, \alpha_N \in [1, 1.5]$

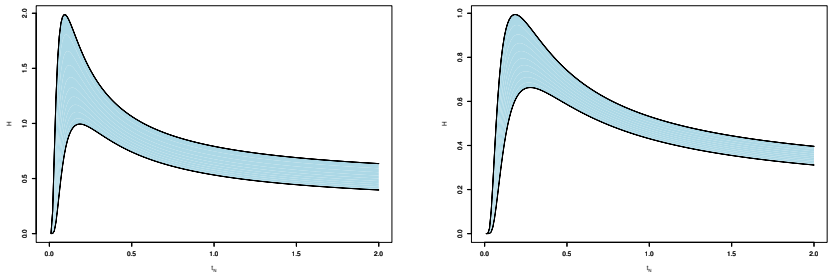

$\alpha = 1.5, \beta_N \in [0.5, 1]$ $\alpha = 1.5, \beta_N \in [1, 1.5]$

Figure 3: The hazard function plots of NBSD against different neutrosophic parameters' values.

of β_N only affect mean and variance, as coefficient of variation, skewness, and kurtosis remain independent of β_N, as shown in Table 1.

Table 2: The properties of NBSD for selected values of neutrosophic parameters.

β_N	α_N	Mean	Variance	Coefficient of variation	Skewness	Kurtosis
$[0.500, 1.000]$	$[0.100, 0.350]$	$[0.502, 1.061]$	$[0.003, 0.141]$	$[0.100, 0.354]$	$[0.300, 1.038]$	$[3.150, 4.775]$
	$[0.500, 0.750]$	$[0.562, 1.281]$	$[0.082, 0.958]$	$[0.509, 0.764]$	$[1.455, 2.056]$	$[6.442, 9.713]$
	$[1.000, 1.500]$	$[0.750, 2.125]$	$[0.562, 8.578]$	$[1.000, 1.378]$	$[2.519, 3.098]$	$[12.852, 17.469]$
	$[2.000, 3.000]$	$[1.500, 5.500]$	$[6.000, 110.250]$	$[1.633, 1.909]$	$[3.402, 3.673]$	$[20.167, 22.724]$
$[1.000, 2.000]$	$[0.100, 0.350]$	$[1.005, 2.122]$	$[0.010, 0.565]$	$[0.100, 0.354]$	$[0.300, 1.038]$	$[3.150, 4.775]$
	$[0.500, 0.750]$	$[1.125, 2.562]$	$[0.328, 3.832]$	$[0.509, 0.764]$	$[1.455, 2.056]$	$[6.442, 9.713]$
	$[1.000, 1.500]$	$[1.500, 4.250]$	$[2.250, 34.312]$	$[1.000, 1.378]$	$[2.519, 3.098]$	$[12.852, 17.469]$
	$[2.000, 3.000]$	$[3.000, 11.000]$	$[24.000, 441.000]$	$[1.633, 1.909]$	$[3.402, 3.673]$	$[20.167, 22.724]$
$[2.000, 3.000]$	$[0.100, 0.350]$	$[2.010, 3.184]$	$[0.041, 1.271]$	$[0.100, 0.354]$	$[0.300, 1.038]$	$[3.150, 4.775]$
	$[0.500, 0.750]$	$[2.250, 3.844]$	$[1.312, 8.622]$	$[0.509, 0.764]$	$[1.455, 2.056]$	$[6.442, 9.713]$
	$[1.000, 1.500]$	$[3.000, 6.375]$	$[9.000, 77.203]$	$[1.000, 1.378]$	$[2.519, 3.098]$	$[12.852, 17.469]$
	$[2.000, 3.000]$	$[6.000, 16.500]$	$[96.000, 992.250]$	$[1.633, 1.909]$	$[3.402, 3.673]$	$[20.167, 22.724]$

5. Neutrosophic parametric estimation

In this section, we present a method for parametric estimation within a neutrosophic framework, where data indeterminacy is represented through interval values. This approach extends the maximum likelihood estimation (MLE) by using neutrosophic intervals, thereby accommodating uncertain data within the likelihood maximization process. We begin by summarizing the conventional MLE for the BSD, as developed by [14], and then detail the neutrosophic maximum likelihood estimation (NMLE) for the NBSD.

5.1. MLE for BSD parameters

The log-likelihood function, derived under the assumption that data follows the BSD, is defined as follows:

$$\begin{aligned} l(\alpha, \beta \mid D) \propto & - n\ln(\alpha) - n\ln(\beta) \\ & + \sum_{i=1}^{n} \ln\left[\left(\frac{\beta}{t_i}\right)^{1/2} + \left(\frac{\beta}{t_i}\right)^{3/2}\right] - \frac{1}{2\alpha^2}\sum_{i=1}^{n}\left(\frac{t_i}{\beta} + \frac{\beta}{t_i} - 2\right), \end{aligned} \tag{9}$$

where $D = \{t_1, \cdots, t_n\}$ represents a random sample from $BS(\alpha, \beta)$.

To maximize (9), we first solve $\frac{\partial}{\partial\alpha} l(\alpha, \beta \mid D) = 0$, yielding

$$\alpha^2 = \left[\frac{s}{\beta} + \frac{\beta}{r} - 2\right], \tag{10}$$

where s and r are the arithmetic and harmonic means of the sample, defined as

$$s = \frac{1}{n}\sum_{i=1}^{n} t_i, \quad r = \left[\frac{1}{n}\sum_{i=1}^{n} t_i^{-1}\right]^{-1}.$$

Differentiating (9) with respect to β and setting it to zero, and then substituting α^2 from (10), we obtain the non-linear equation

$$\beta^2 - \beta(2r + K(\beta)) + r(s + K(\beta)) = 0, \tag{11}$$

where

$$K(x) = \left[\frac{1}{n}\sum_{i=1}^{n} (x + t_i)^{-1}\right]^{-1}, \quad x \geq 0.$$

Once $\hat{\beta}$ is computed, the MLE of α is given by

$$\hat{\alpha} = \left[\frac{s}{\hat{\beta}} + \frac{\hat{\beta}}{r} - 2\right]^{1/2}. \tag{12}$$

It has been established that the MLEs of α and β are consistent estimators, noting that for sample size $n = 1$, the MLEs do not exist, but are unique for $n > 1$ as shown in [14].

5.2. NMLE for NBSD parameters

To incorporate data uncertainty, we extend the maximum likelihood framework by defining each observation as an interval $t_{Ni} = (t_{Li}, t_{Ui})$ for $i = 1, \cdots, n$. Accordingly, the neutrosophic likelihood function is defined as:

$$l(\alpha_N, \beta_N \mid D_N) \propto \prod_{i=1}^{n} f(t_{Ni}; \alpha_N, \beta_N), \tag{13}$$

where $D_N = \{t_{N1}, \cdots, t_{Nn}\}$ represents a sample from $NBS(\alpha_N, \beta_N)$.

In neutrosophic statistics, indeterminacy is handled by optimizing the likelihood function over the interval space of the data. Therefore, to derive the NMLEs, we perform a two-step interval maximization:

- **Step 1: Define the Indeterminate Space.** Define the space of all possible observations $S_N = \prod_{i=1}^{n} t_{Ni}$, where each observation interval t_{Ni} contributes to the overall parameter uncertainty.

- **Step 2: Compute Interval Boundaries.** For each $\underline{t} = (t_1, \cdots, t_n) \in S_N$, compute the MLEs of parameters based on equations (11) and (12). The NMLEs are then obtained by determining the minimum and maximum estimates across all possible values of $\underline{t}$.

Let $\Theta(\underline{t}) = \underset{(\alpha,\beta)}{\operatorname{argmax}}\, l(\alpha, \beta \mid \underline{t})$ denote the set of parameter values that maximize the likelihood function for a given interval observation $\underline{t} \in S_N$. Thus, the NMLEs can be computed as follows:

$$\begin{aligned} \hat{\alpha}_N &= \left(\min_{\underline{t} \in S_N} \{\hat{\alpha} \mid \hat{\alpha} \in \Theta(\underline{t})\}, \max_{\underline{t} \in S_N} \{\hat{\alpha} \mid \hat{\alpha} \in \Theta(\underline{t})\} \right) \\ \hat{\beta}_N &= \left(\min_{\underline{t} \in S_N} \left\{\hat{\beta} \mid \hat{\beta} \in \Theta(\underline{t})\right\}, \max_{\underline{t} \in S_N} \left\{\hat{\beta} \mid \hat{\beta} \in \Theta(\underline{t})\right\} \right) \end{aligned} \tag{14}$$

The non-linear optimization in (14) is implemented by generating a large number of data vectors within the admissible region S_N, where each vector is formed by independently sampling values from the observed intervals. For each generated vector, the likelihood function is maximized with respect to the parameters, and the corresponding MLEs are recorded. The NMLEs are finally derived by extracting the extremal values of these estimates across all evaluated instances.

This interval-based approach provides robust parameter estimates in the presence of data uncertainty, as the NMLEs reflect both the lower and upper bounds of the parameter estimates within the indeterminate data space.

6. Simulation study

In this section, a simulation study is presented to evaluate the performance of the NMLEs in the NBSD. Unlike classical statistics, which provide point estimates, the NBSD offers interval-valued estimates that capture both randomness and inherent uncertainty. This approach is particularly useful when precise data are unavailable or subject to variability.

According to [10], a neutrosophic variable is defined as $T_N = T + I$, where T is the determined part and I represents the uncertain part. In this framework, I can either be a constant value capturing fixed uncertainty or modeled as a uniform distribution $I \sim U(-\epsilon, \epsilon)$ to represent variable uncertainty. This approach enables the model to integrate both static and dynamic uncertainties, enhancing the accuracy of real-world estimations.

For this study, we generated $N = 1000$ random samples of sizes $n = 30, 50, 100,$ and 200 from the NBSD. For each observation T_N, uncertainty was introduced using

additive uniform noise $I \sim U(-\epsilon, \epsilon)$, with values $\epsilon = 0.005, 0.01$, and 0.1. This method captures variability and reflects the model's flexibility in adapting to uncertain data.

In the simulation, NMLEs were calculated using (14) to assess performance. To evaluate accuracy, we computed the neutrosophic mean squared error (NMSE), neutrosophic average estimates (NAE), and neutrosophic average biases (NAB). For each parameter, NMSE was obtained by averaging the squared differences between the estimated and true interval bounds over N replications. NAE and NAB were similarly computed based on the average values of the estimated bounds and their deviations from the true bounds, respectively, across all simulations. Table 3 shows that NMSE decreases with larger sample sizes, confirming that the NBSD performs reliably with more data and is effective in reducing estimation error. Furthermore, as ϵ increases, the parameter intervals expand, demonstrating the model's adaptability to higher levels of uncertainty. This aligns with the expected behavior under the interval neutrosophic framework, providing more reliable estimates in the face of data indeterminacy.

For instance, with $\alpha = 0.5$, $\beta = 1.5$, and $n = 200$, the NAE values for α_N are:

$$\epsilon = 0.005 : [0.498, 0.499], \quad \epsilon = 0.01 : [0.497, 0.499], \quad \epsilon = 0.1 : [0.490, 0.510].$$

To enhance reproducibility, the R code used in this study, including functions for data generation, parameter estimation, and optimization procedures, is publicly available in this GitHub repository. The repository includes comments and documentation to facilitate use and allow readers to reproduce our results or extend the method to related applications.

7. Comparative evaluation of estimation strategies

Since the primary aim of this study is to propose a more accurate method for analyzing interval-valued data, it is essential to evaluate the extent to which the proposed approach outperforms simpler alternatives. In many previous studies, interval data have typically been analyzed by relying solely on their endpoints, without incorporating the internal structure of the intervals into the estimation process. Such endpoint-based formulations or estimation frameworks can be found, for example, in [3, 5, 16]. While such simplifications are common and computationally convenient, they may reduce the accuracy and coverage of parameter estimates. Given that the NBSD is particularly sensitive to its shape parameter, and that its practical applications (e.g., in fatigue or reliability analysis) demand precise inference, it is important to examine whether relying solely on interval bounds may lead to loss of information, and to assess the benefits of a full-interval estimation approach. The following simulation study evaluates the performance of both approaches.

Table 3: NMLEs simulation results

		NAE		NAB		NMSE	
ϵ	n	$\hat{\alpha}_N$	$\hat{\beta}_N$	$\hat{\alpha}_N$	$\hat{\beta}_N$	$\hat{\alpha}_N$	$\hat{\beta}_N$
				$\alpha = 0.25$, $\beta = 1$			
0.005	30	[0.242, 0.243]	[0.999, 1.002]	[-0.008, -0.007]	[-0.001, 0.002]	[0.033, 0.033]	[0.047, 0.047]
	50	[0.248, 0.248]	[1.000, 1.003]	[-0.002, -0.002]	[0.000, 0.003]	[0.025, 0.025]	[0.034, 0.034]
	100	[0.248, 0.248]	[1.000, 1.003]	[-0.002, -0.002]	[0.000, 0.003]	[0.018, 0.018]	[0.025, 0.025]
	200	[0.249, 0.249]	[0.998, 1.000]	[-0.001, -0.001]	[-0.003, 0.000]	[0.013, 0.013]	[0.018, 0.017]
0.01	30	[0.242, 0.244]	[0.998, 1.003]	[-0.008, -0.007]	[-0.002, 0.003]	[0.033, 0.033]	[0.047, 0.047]
	50	[0.247, 0.249]	[0.999, 1.004]	[-0.003, -0.001]	[-0.001, 0.004]	[0.025, 0.025]	[0.034, 0.035]
	100	[0.247, 0.249]	[0.999, 1.004]	[-0.003, -0.001]	[-0.001, 0.004]	[0.018, 0.018]	[0.025, 0.025]
	200	[0.249, 0.250]	[0.996, 1.001]	[-0.002, 0.000]	[-0.004, 0.001]	[0.013, 0.013]	[0.018, 0.017]
0.1	30	[0.237, 0.254]	[0.974, 1.026]	[-0.013, 0.004]	[-0.026, 0.026]	[0.035, 0.033]	[0.055, 0.054]
	50	[0.243, 0.259]	[0.975, 1.027]	[-0.007, 0.009]	[-0.025, 0.027]	[0.026, 0.028]	[0.043, 0.044]
	100	[0.244, 0.258]	[0.975, 1.027]	[-0.006, 0.008]	[-0.025, 0.027]	[0.019, 0.020]	[0.035, 0.036]
	200	[0.245, 0.259]	[0.972, 1.024]	[-0.005, 0.009]	[-0.028, 0.024]	[0.013, 0.016]	[0.033, 0.030]
				$\alpha = 0.5$, $\beta = 1.5$			
0.005	30	[0.484, 0.485]	[1.503, 1.506]	[-0.016, -0.015]	[0.003, 0.006]	[0.066, 0.066]	[0.139, 0.139]
	50	[0.495, 0.496]	[1.504, 1.507]	[-0.005, -0.004]	[0.004, 0.007]	[0.051, 0.051]	[0.101, 0.101]
	100	[0.495, 0.496]	[1.503, 1.506]	[-0.005, -0.004]	[0.003, 0.006]	[0.036, 0.035]	[0.072, 0.072]
	200	[0.498, 0.499]	[1.495, 1.498]	[-0.002, -0.001]	[-0.005, -0.002]	[0.026, 0.026]	[0.051, 0.051]
0.01	30	[0.484, 0.486]	[1.502, 1.507]	[-0.016, -0.014]	[0.002, 0.007]	[0.066, 0.066]	[0.139, 0.139]
	50	[0.495, 0.497]	[1.503, 1.509]	[-0.005, -0.003]	[0.003, 0.009]	[0.051, 0.051]	[0.101, 0.101]
	100	[0.495, 0.497]	[1.502, 1.508]	[-0.005, -0.003]	[0.002, 0.008]	[0.036, 0.035]	[0.072, 0.073]
	200	[0.497, 0.499]	[1.494, 1.500]	[-0.003, -0.001]	[-0.006, 0.000]	[0.026, 0.026]	[0.051, 0.051]
0.1	30	[0.477, 0.496]	[1.475, 1.532]	[-0.024, -0.004]	[-0.025, 0.032]	[0.067, 0.066]	[0.142, 0.143]
	50	[0.488, 0.507]	[1.476, 1.534]	[-0.013, 0.007]	[-0.024, 0.034]	[0.051, 0.053]	[0.104, 0.107]
	100	[0.487, 0.507]	[1.475, 1.533]	[-0.013, 0.007]	[-0.025, 0.033]	[0.037, 0.037]	[0.077, 0.079]
	200	[0.490, 0.510]	[1.467, 1.525]	[-0.010, 0.010]	[-0.033, 0.025]	[0.027, 0.029]	[0.061, 0.057]

To this end, we conducted a simulation-based comparison between the proposed method and a simplified estimation strategy that relies only on interval bounds. Simulations were carried out for three parameter configurations: $(\alpha, \beta) \in \{(0.1, 1), (0.1, 2), (0.2, 3)\}$. For each setting, two levels of imprecision were considered, namely $\epsilon \in \{0.05,\ 0.1\}$, and three different sample sizes: $n \in \{20,\ 50,\ 100\}$. For each combination $(\alpha, \beta, \epsilon, n)$, we performed $N = 1000$ replications.

The following two estimation methods were compared:

- Method A (Proposed): uses the full interval in the estimation procedure.
- Method B (Alternative): treats the lower and upper bounds of each interval as separate observations and applies classical BS estimation independently.

For each method, the Empirical Coverage Rate (ECR) was calculated as the proportion of replications in which the true value of a parameter was captured within its

corresponding estimated interval. ECR serves as a key diagnostic metric for assessing the reliability of interval estimates: higher coverage indicates greater alignment between the estimated uncertainty and the true parameter variability.

The results are summarised in Table 4. Across all parameter configurations and sample sizes, Method A consistently yielded substantially higher coverage for α, clearly demonstrating the benefit of incorporating full interval information when estimating parameters sensitive to data imprecision. In contrast, Method B, by relying only on endpoints, often underestimates the true variability and results in lower coverage for α, thereby reducing the credibility of the inferred uncertainty. For β, both methods yielded similar ECR values. This is because the MLE of β is monotonic with respect to the data, so that its value is primarily determined by the interval bounds, and the internal distribution of values within the intervals has no effect on its estimation. These findings highlight that, in situations where the MLE is not monotonic with respect to the data, disregarding the internal structure of intervals can lead to misleading uncertainty quantification.

Table 4: ECR comparison of interval and endpoint-based methods

				Model A				Model B			
				NAE		ECR		NAE		ECR	
ϵ	α	β	n	$\hat{\alpha}_N$	$\hat{\beta}_N$	$\hat{\alpha}_N$	$\hat{\beta}_N$	$\hat{\alpha}_N$	$\hat{\beta}_N$	$\hat{\alpha}_N$	$\hat{\beta}_N$
0.05	0.1	1	20	[0.092, 0.103]	[0.987, 1.012]	27.3	41.3	[0.096, 0.100]	[0.987, 1.012]	9.1	41.3
			50	[0.096, 0.103]	[0.987, 1.012]	30.7	63.5	[0.098, 0.101]	[0.987, 1.012]	10.9	63.5
			100	[0.098, 0.103]	[0.987, 1.012]	27.5	77.6	[0.099, 0.102]	[0.987, 1.012]	13.7	77.6
0.1	0.1	1	20	[0.089, 0.113]	[0.975, 1.026]	50.5	73.1	[0.097, 0.104]	[0.975, 1.026]	15.9	73.1
			50	[0.096, 0.112]	[0.974, 1.024]	53.8	91.9	[0.101, 0.107]	[0.974, 1.024]	20.2	91.9
			100	[0.099, 0.110]	[0.975, 1.025]	47.4	98.3	[0.102, 0.107]	[0.975, 1.025]	23.1	98.3
0.05	0.1	2	20	[0.093, 0.099]	[1.987, 2.012]	12.9	18.8	[0.095, 0.097]	[1.987, 2.012]	3.9	18.8
			50	[0.097, 0.101]	[1.988, 2.013]	15.8	34.9	[0.098, 0.099]	[1.988, 2.013]	5.8	34.9
			100	[0.098, 0.101]	[1.988, 2.013]	17.8	48.4	[0.099, 0.100]	[1.988, 2.013]	9.1	48.4
0.1	0.1	2	20	[0.092, 0.103]	[1.977, 2.027]	27.6	41.3	[0.096, 0.099]	[1.977, 2.027]	7.6	41.3
			50	[0.096, 0.103]	[1.976, 2.026]	29.1	60.6	[0.098, 0.101]	[1.976, 2.026]	9.5	60.6
			100	[0.098, 0.103]	[1.974, 2.024]	32.1	79.4	[0.099, 0.102]	[1.974, 2.024]	16.9	79.4
0.05	0.2	3	20	[0.190, 0.194]	[2.983, 3.009]	5.5	8.1	[0.191, 0.193]	[2.983, 3.009]	2.3	8.1
			50	[0.196, 0.199]	[2.982, 3.008]	5.6	12.6	[0.196, 0.198]	[2.982, 3.008]	4.0	12.6
			100	[0.197, 0.199]	[2.990, 3.015]	5.6	17.0	[0.197, 0.199]	[2.990, 3.015]	4.4	17.0
0.1	0.2	3	20	[0.188, 0.196]	[2.977, 3.027]	9.5	14.2	[0.190, 0.194]	[2.977, 3.027]	4.3	14.2
			50	[0.195, 0.200]	[2.977, 3.028]	9.7	23.3	[0.196, 0.199]	[2.977, 3.028]	5.7	23.3
			100	[0.197, 0.201]	[2.974, 3.025]	10.6	31.6	[0.197, 0.201]	[2.974, 3.025]	9.3	31.6

8. Applications

8.1. Pseudo neutrosophic data

In this section, we apply the NBS model to a real dataset to demonstrate its practical application. The dataset, comprising 101 observations, represents the fatigue life of 6061-T6 aluminum coupons. These coupons were cut parallel to the rolling direction and subjected to oscillations at a frequency of 18 cycles per second (cps), with each experiencing a maximum stress per cycle of 31,000 psi. The dataset is presented in Table 5.

Table 5: Fatigue life of 6061-T6 aluminium coupons

70	90	96	97	99	100	103	104	104	105	107	108	108	108	109	109	112	112	113	114	114	114
116	119	120	120	120	121	121	123	124	124	124	124	124	128	128	129	129	130	130	130	131	131
131	131	131	132	132	132	133	134	134	134	134	134	136	136	137	138	138	138	139	139	141	141
142	142	142	142	142	142	144	144	145	146	148	148	149	151	151	152	155	156	157	157	157	157
158	159	162	163	163	164	166	166	168	170	174	196	212									

According to [14], the point estimates for the parameters of the classical BS model are

$$\hat{\alpha} = 0.170385, \quad \hat{\beta} = 131.818792.$$

To extend the analysis into the neutrosophic framework, we introduce varying levels of indeterminacy using the parameter ϵ. The precise dataset serves as the basis for creating neutrosophic datasets, where each ϵ value introduces a specific degree of uncertainty. We consider $T_N = T + \epsilon$ and use $\epsilon = 0, 0.001, 0.01, 0.1,$ and 1 to reflect different levels of indeterminacy. When $\epsilon = 0$, the data remains precise, reflecting a classical scenario. As ϵ increases, the data captures increasing levels of uncertainty, aligning with the neutrosophic concept.

Using the transformed datasets, we estimate the parameters α and β of the NBS model across the different ϵ-values. These estimates, along with corresponding Akaike's Information Criterion (AIC) and Bayesian Information Criterion (BIC), are presented in Table 6. These metrics, presented as intervals, capture the range of variability introduced by the neutrosophic framework, with each interval representing the absolute minimum and maximum values identified within the transformed datasets.

Given that the distribution's parameters are unknown, we assess the model's fit using the modified Kolmogorov-Smirnov (KS) test, as demonstrated by [17]. The modified KS statistic for a given dataset $t_1, \ldots, t_n$ following a distribution F is defined as

$$KS^* = \left[\sqrt{n} - 0.01 + \frac{0.85}{\sqrt{n}}\right] \max\left\{D^+, D^-\right\}, \tag{15}$$

where

$$D^+ = \max_{j=1,\ldots,n}\{j/n - u_j\}, \quad \text{and} \quad D^- = \max_{j=1,\ldots,n}\{u_j - [j-1]/n\}.$$

The step-by-step procedure for calculating the u_j values is outlined in Algorithm 1. This adjustment, which is specifically designed for skewed distributions, is particularly suitable for our dataset, which consists of fatigue life data. Since the BSD also exhibits skewness, the modified KS test is the most appropriate method for this scenario, as it effectively handles the asymmetry in the data.

Algorithm 1 Calculating u_js in modified KS statistic

1. Calculate MLEs for α_N and β_N; $\hat{\alpha}_N$ and $\hat{\beta}_N$.
2. Sort the dataset t_i in ascending order and compute the corresponding CDF values of the BSD as $v_i = F(t_i; \hat{\alpha}_N, \hat{\beta}_N)$.
3. Transform v_i to y_i using $y_i = \Phi^{-1}(v_i)$, where Φ is the standard normal CDF and Φ^{-1} is its inverse.
4. Compute $u_i = \Phi\left\{(y_i - \bar{y})/s_y\right\}$, where $\bar{y} = n^{-1}\sum_{i=1}^{n} y_i$ and $s_y^2 = (n-1)^{-1}\sum_{i=1}^{n}(y_i - \bar{y})^2$.

For neutrosophic datasets, we extend this approach by using the modified KS test to identify the absolute extrema of KS statistics. This involves applying the test to transformed neutrosophic data, establishing boundaries that encompass dataset indeterminacy. These interval-based KS statistics capture the full range of uncertainty represented within the neutrosophic framework, offering deeper insights into model fit under varying degrees of indeterminacy.

The results from the transformed datasets and the corresponding parameter estimates are presented in Table 6. The interval values for AIC and BIC provide insight into how well the neutrosophic model fits the data at different uncertainty levels. As the level of uncertainty decreases (i.e., smaller ϵ-values), the neutrosophic model converges toward the behavior of classical statistical models, which assume precise data. In the case of $\epsilon = 0$, this corresponds specifically to the BS model. Conversely, with larger ϵ-values, the model captures more uncertainty, demonstrating the flexibility and robustness of the neutrosophic approach.

8.2. Environmental dataset

Neutrosophic logic is particularly useful in modelling and analysing environmental datasets, where uncertainties and incomplete information are common. This includes

Table 6: Parameter estimates and goodness-of-fit statistics for the aluminum coupons dataset.

ϵ	Parameter	Estimate	Log-likelihood	AIC	BIC	KS*
0	$\hat{\alpha}_N$	0.170	-457.271	918.541	933.002	0.857
	$\hat{\beta}_N$	131.819				
0.001	$\hat{\alpha}_N$	[0.170, 0.170]	[-457.271, -457.269]	[918.539, 918.543]	[933.000, 933.003]	[0.857, 0.857]
	$\hat{\beta}_N$	[131.817, 131.819]				
0.01	$\hat{\alpha}_N$	[0.170, 0.170]	[-457.278, -457.264]	[918.527, 918.557]	[932.988, 933.017]	[0.857, 0.857]
	$\hat{\beta}_N$	[131.808, 131.829]				
0.1	$\hat{\alpha}_N$	[0.170, 0.170]	[-457.350, -456.2038]	[918.407, 918.700]	[932.868, 933.161]	[0.857, 0.858]
	$\hat{\beta}_N$	[131.717, 131.920]				
1	$\hat{\alpha}_N$	[0.169, 0.172]	[-458.093, -456.636]	[917.273, 920.186]	[931.733, 934.647]	[0.854, 0.860]
	$\hat{\beta}_N$	[130.802, 132.835]				

climate modelling, ecological studies, and environmental risk assessments. Environmental data often exhibit uncertainties due to factors such as measurement errors, variability, and missing information. Neutrosophic statistics effectively address these challenges by modelling uncertainty, offering a more nuanced understanding of the data.

For example, the neutrosophic framework can account for indeterminacy in climate model parameters, deal with incomplete observational data, and handle uncertain parameters in hydrological models. These models often involve uncertainties about rainfall, runoff, and other environmental variables. In environmental emergencies or disasters, where information is rapidly changing and incomplete, the neutrosophic approach provides robust tools for dynamic analysis.

To illustrate the computational methodology of the proposed NBS model, we use an environmental dataset analyzed by [8], which focuses on yearly nitrogen oxides emissions in Denmark from 1990 to 2018. This dataset has been compiled by the United Nations Statistics Division (UNSD) and is available on their website. The dataset is shown in Table 7.

Table 7: Nitrogen oxides emissions dataset in Denmark (1990–2018).

$[304.12, 307.82], 355.34, 310.93, 309.47, [309.12, 312.10], 292.80, 327.49, 280.33, 259.99,$
$[238.19, 242.45], 229.98, 226.77, 223.57, 233.12, 216.37, 208.16, [206.30, 209.14], 193.44,$
$177.31, 157.88, 153.18, 143.93, 132.78, 127.87, 118.28, 116.75, 116.96, 114.21, [106.86, 110.62]$

This dataset provides emissions as intervals (e.g., $[304.12, 307.82]$, $[309.12, 312.10]$), reflecting measurement uncertainty. Using (15), we first calculate the KS* value and obtain the corresponding p-value through Monte Carlo (MC) simulations. Classical models, such as the BS model, struggle to handle such interval-based data, leading to ambiguous outcomes and would ignore the core aspects of indeterminacy. However,

neutrosophic models allow us to compare the performance of various models under uncertainty. Here, we compare the performance of the NBSD, neutrosophic gamma (NG), and neutrosophic log-normal (NLN) models. Table 8 summarizes the results. All three models exhibit p-values higher than the significance level ($\alpha = 0.05$), indicating an adequate fit to the data. Thus, we select the model with the lowest AIC and BIC values, as it offers the best trade-off between goodness-of-fit and model complexity. The NBSD model provides the lowest AIC and BIC values, indicating superior performance among the tested models.

Table 8: Parameter estimates and goodness-of-fit statistics for the environmental dataset.

Model	MLEs	Log-likelihood	AIC	BIC	KS*	p-value
NBSD	$\hat{\alpha}_N = [0.370, 0.373]$ $\hat{\beta}_N = [199.642, 200.267]$	[-165.759, -165.586]	[335.173, 335.519]	[344.642, 344.988]	[0.659, 0.694]	[0.278, 0.363]
NLND	$\hat{\mu}_N = [5.299, 5.302]$ $\hat{\sigma}_N = [0.367, 0.370]$	[-166.018, -165.747]	[335.494, 336.035]	[344.963, 345.504]	[0.658, 0.693]	[0.280, 0.365]
NGD	$\hat{\alpha}_N = [0.078, 0.078]$ $\hat{\sigma}_N = [2722.338, 2731.369]$	[-234.619, -234.520]	[473.040, 473.238]	[482.510, 482.707]	[0.573, 0.590]	[0.531, 0.589]

The NBSD model achieves the best fit for this environmental dataset, effectively capturing interval-based uncertainties in emissions data.

9. Comparison with an alternative model

In this section, we focus on evaluating the performance of our proposed neutrosophic model on real-world interval-valued datasets, comparing its results with those of an existing NBSD model. We reanalyze the two real-world datasets introduced in [13], namely alloy melting points and battery lifetimes, by applying our proposed method to directly estimate the parameters from the full interval-valued observations. These datasets, presented in Table 9, represent naturally imprecise measurements and serve as practical examples of applying neutrosophic modelling under uncertainty.

The results, summarized in Table 10, indicate that our method consistently achieves lower AIC and BIC values compared to the alternative model, for both datasets. This suggests a more efficient statistical fit and stronger representation of the underlying uncertainty. By preserving the interval structure of the data, our approach avoids oversimplification and enables a more faithful and robust inference. These outcomes highlight the practical advantages of our neutrosophic framework when dealing with imprecise and uncertain information in real-world contexts.

Table 9: Interval-valued data used in Applications 1 and 2.

Application 1: Alloy melting points
$[545.5, 563.3], [511.6, 529.4], [503.5, 523.1], [449.2, 470.1], [489.0, 506.7], [479.1, 495.6], [467.9, 495.3],$ $[495.6, 520.9], [472.8, 496.9], [519.1, 542.9], [484.0, 505.4], [525.9, 550.7], [500.9, 517.7], [483.0, 499.2],$ $[480.0, 500.6], [499.6, 516.8], [515.1, 535.0], [464.4, 489.3]$
Application 2: Battery lifetimes
$[2.9, 3.99], [5.24, 7.2], [6.56, 9.02], [7.14, 9.82], [11.6, 15.96], [12.14, 16.69], [12.65, 17.4], [13.24, 18.21]$ $[13.67, 18.79], [13.88, 19.09], [15.64, 21.51], [17.05, 23.45], [17.4, 23.93], [17.8, 24.48], [19.01, 26.14], [19.34, 26.59]$ $[23.13, 31.81], [23.34, 32.09], [26.07, 35.84], [30.29, 41.65], [43.97, 60.46], [48.09, 66.13], [73.48, 98.04]$

Table 10: Model comparison using AIC and BIC for both applications.

Application	Model	MLEs	Log-likelihood	AIC	BIC
Application 1	Our proposed NBS model	$\hat{\alpha}_N = [0.038, 0.055]$ $\hat{\beta}_N = [493.125, 513.877]$	[-85.344, -78.479]	[160.958, 174.687]	[168.520, 182.249]
	The alternative NBS model	$\hat{\alpha}_N = [0.002, 0.002]$ $\hat{\beta}_N = [0.004, 0.005]$	[-1499.762, -1464.573]	[5860.827, 5897.769]	[5864.169, 5904.826]
Application 2	Our proposed NBS model	$\hat{\alpha}_N = [0.701, 0.826]$ $\hat{\beta}_N = [15.964, 21.897]$	[-96.144, -88.953]	[181.906, 196.288]	[190.448, 204.830]
	The alternative NBS model	$\hat{\alpha}_N = [0.046, 0.063]$ $\hat{\beta}_N = [0.755, 0.758]$	[-2299.823, -2201.847]	[4407.694, 4503.000]	[4409.474, 4505.427]

10. Conclusion

This study presents the Neutrosophic Birnbaum-Saunders Distribution (NBSD), extending the Birnbaum-Saunders Distribution (BSD) in a neutrosophic framework to effectively handle data characterized by uncertainty and indeterminacy. The NBSD provides an approach that fully preserves the range of data variability, making it particularly valuable in engineering applications, such as reliability assessment and material fatigue analysis, where accuracy and completeness of information are critical.

A distinctive strength of the NBSD lies in its ability to capture the full range of interval-based values without compromise. Unlike simplified approaches that rely solely on interval bounds or consider a linear combination of boundaries, our method provides estimates that are consistent with the internal structure of the intervals, thereby preventing information loss during the estimation process. This integrity offers practitioners a more reliable tool for life cycle assessments and decision-making, especially in high-stakes environments.

In simulations, the NBSD demonstrated its capacity to maintain robust interval-based estimates, allowing for a nuanced understanding of variability. While it may require slightly more time compared to endpoint-based simplifications, it provides a substantially richer representation of uncertainty. The method retains structural flexibility and is applicable to a wide range of continuous distributions. In this study, its effectiveness has been demonstrated through applications to multiple models, with particularly promising results observed for the NBSD (see Section 8.2).

Our model is relevant across fields requiring rigorous uncertainty quantification, including but not limited to engineering and environmental monitoring, thus broadening the BSD's applicability. For future studies, we aim to extend the NBSD framework to accommodate more flexible distributions like Generalized NBSD and alternative inferential approaches, such as Bayesian methods, in order to further enhance the model's efficiency and robustness in the presence of indeterminate data. With R code provided for reproducibility, this work supports further exploration and adaptation across varied industries, where interval-based reliability models are increasingly valuable.

Declaration of competing interest

The authors declare that they have no known competing financial interests or personal relationships that could have appeared to influence the work reported in this paper.

Acknowledgments

Andriette Bekker and Mohammad Arashi acknowledge the support of the National Research Foundation (NRF) of South Africa (SA), ref. SRUG2204203865 nr. 120839 and ref. RA211204653274 nr. 151035.

Filipe J. Marques' work was supported by national funds through FCT - Fundação para a Ciência e a Tecnologia, I.P., under the scope of the projects UIDB/00297/2020 (https://doi.org/10.54499/UIDB/00297/2020) and UIDP/00297/2020 (https://doi.org/10.54499/UIDP/00297/2020) (Center for Mathematics and Applications).

The authors would like to thank the Editor-in-Chief and the reviewers for their valuable comments and suggestions which helped to improve the quality of this manuscript.

Author Contributions

Mansooreh Razmkhah: Conceptualization, Methodology, Coding, Formal Analysis, Investigation, Writing - Original Draft, Visualization.

Mohammad Arashi: Conceptualization, Investigation, Visualization, Supervision, Review & Editing.

Andriette Bekker: Conceptualization, Investigation, Visualization, Supervision, Review & Editing.

Filipe J. Marques: Conceptualization, Investigation, Visualization, Review & Editing.

References

[1] F. Smarandache, Introduction to Neutrosophic Statistics, Sitech & Education Publishing, 2014.

[2] R. Alhabib, M.M. Ranna, H. Farah, A.A. Salama, Some neutrosophic probability distributions, Neutrosophic Sets Syst. 22 (2018) 30–38.

[3] K.F.H. Alhasan, F. Smarandache, Neutrosophic Weibull distribution and neutrosophic family Weibull distribution, Neutrosophic Sets Syst. 28 (2019) 191–199.

[4] F. S. Alduais, Z. Khan, Development of Neutrosophic Gamma Distribution for Modeling Neonatal Mortality Data, Neutrosophic Sets Syst. 79(1) (2025) 48.

[5] M. Norouzirad, G.S. Rao, D. Mazarei, Neutrosophic generalized Rayleigh distribution with application, Neutrosophic Sets Syst. 58 (1) (2023) 15.

[6] F. Shah, M. Aslam, Z. Khan, M. Almazah, F.S. Alduais, et al., On neutrosophic extension of the Maxwell model: properties and applications, J. Funct. Spaces 2022, article ID 4536260 (2022).

[7] M. Ahsan-ul Haq, Neutrosophic Kumaraswamy distribution with engineering application, Neutrosophic Sets Syst. 49 (2022) 269–276.

[8] Z. Khan, A. Amin, S.A. Khan, M. Gulistan, Statistical development of the neutrosophic log-normal model with application to environmental data, Neutrosophic Sets Syst. 47 (1) (2021) 1.

[9] G.S. Rao, M. Norouzirad, D. Mazarei, Neutrosophic generalized exponential distribution with application, Neutrosophic Sets Syst. 55 (1) (2023) 471–485.

[10] R.A. Khan Sherwani, M. Naeem, M. Aslam, M.A. Raza, S. Abbas, et al., Neutrosophic beta distribution with properties and applications, Neutrosophic Sets Syst. 41 (1) (2021) 12.

[11] N.I. Eassa, H.M. Zaher, N.A.A. El-Magd, Neutrosophic generalized Pareto distribution, Math. Stat. 11 (2023) 827–833.

[12] F. Jamal, S. Shafiq, M. Aslam, S. Khan, Z. Hussain, Q. Abbas, Modeling COVID-19 data with a novel neutrosophic Burr-III distribution, Sci. Rep. 14 (1) (2024) 10810.

[13] M.K. Hassan, M. Aslam, Birnbaum-Saunders distribution for imprecise data: statistical properties, estimation methods, and real life applications, Sci. Rep. 14 (2024) 6955.

[14] N. Balakrishnan, D. Kundu, Birnbaum-Saunders distribution: A review of models, analysis, and applications, Appl. Stoch. Models Bus. Ind. 35 (1) (2019) 4–49.

[15] R Core Team, *optim: General-purpose optimization*, R Documentation, Available at: `https://www.rdocumentation.org/packages/stats/topics/optim`.

[16] Z. Khan, Z.T. Kosztyan, neutrostat: Neutrosophic Statistical Distributions, R package version 0.1.0, 2024. Available at: `https://CRAN.R-project.org/package=neutrostat`.

[17] M. Barros, R. Ospina, A. Tsuyuguchi, Goodness-of-fit tests for the Birnbaum-Saunders distribution with censored reliability data, IEEE Trans. Reliab. 63(2) (2014) 543–554.